ACS Biomaterials SCIENCE & ENGINEERING

Article

pubs.acs.org/journal/abseba

Collagen Fibril Structure and Strength in Acellular Dermal Matrix Materials of Bovine, Porcine, and Human Origin

Hannah C. Wells,[†] Katie H. Sizeland,[†] Nigel Kirby,[‡] Adrian Hawley,[‡] Stephen Mudie,[‡] and Richard G. Haverkamp*[,†]

[†]School of Engineering and Advanced Technology, Massey University, Private Bag 11222, Palmerston North, New Zealand

[‡]Australian Synchrotron, 800 Blackburn Road, Clayton, Melbourne, Victoria, Australia

ABSTRACT: Strength is an important characteristic of acellular dermal matrix (ADM) materials used for surgical scaffolds. Strength depends on the material's structure, which may vary with the source from which the product is produced, including species and animal age. Here, variations in the physical properties and structures of ADM materials from three species are investigated: bovine (fetal and neonatal), porcine, and human materials. Thickness normalized, the bovine materials have a similar strength (tear strength of 75−124 N/m) to the human material (79 N/m), and these are both stronger than the porcine material (43 N/m). Thickness-normalized tensile strengths were similar among all species (18−34 N/mm^2 for bovine although higher in fetal material, 18 N/mm^2 for human and 21 N/mm^2 for porcine). Structure is investigated with synchrotron-based small-angle X-ray scattering (SAXS) for collagen fibril orientation index (OI) and scanning electron microscopy (SEM). SEM reveals a more open structure in bovine ADM than in the porcine and human material. A correlation is found between OI and thickness-normalized tear strength in neonatal bovine material measured with the X-rays edge-on to the sample, but this relationship does not extend across species. The collagen fibril arrangement, viewed perpendicular to the surface, varies between species, with the human material having a unimodal distribution and rather isotropic (OI 0.08), the porcine being strongly bimodal and rather highly oriented (OI 0.61), the neonatal bovine between these two extremes with a bimodal distribution tending toward isotropic (OI 0.14−0.21) and the fetal bovine material being bimodal and less isotropic than neonatal (OI 0.24). The OI varies less through the thickness of the porcine and human materials than through the bovine materials. The similarities and differences in structure may inform the suitability of these materials for particular surgical applications.

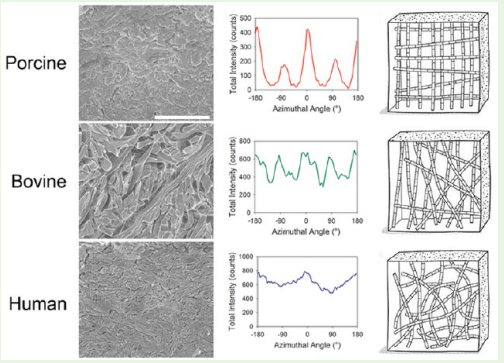

KEYWORDS: *collagen, scaffold, ADM, ECM, strength, orientation*

INTRODUCTION

Scaffold materials are required when a tissue is being reinforced or replaced in a number of reconstructive surgical procedures. These materials must meet a range of requirements such as being immunologically compatible with the body, be readily incorporated into living tissue, have sufficient strength to perform the task, and have appropriate elastic properties. These scaffold materials may be synthesized from a variety of materials[1] or produced by decellurization of native materials. Extracellular matrix materials (ECM) derived from a wide variety of tissues have been successfully used a scaffolds.[2] ECM materials derived from dermal tissues are commercially available and are produced from a variety of species including porcine, bovine, and human dermal tissue. The physical properties of materials manufactured from different source materials differ, yet there is an incomplete understanding of these differences and the structural characteristics that lead to the differences in strength.

The mechanical properties of collagen tissue materials are due in part to the highly fibrillar nature of type I collagen[3,4] and the tissue's ability to respond to imposed stresses.[5] Factors that have been considered as contributing to the strength of collagenous tissue materials include the structure of the collagen (*d*-spacing, collagen type), the nature of the cross-linking between collagen, collagen fibril diameter and collagen orientation. The fibril arrangement can be described in terms of orientation direction and spread. Collagen orientation (quantified as orientation index, OI) has been investigated in the cornea,[6] heart valve tissue,[7] pericardium,[8,9] bladder tissue,[10] skin,[11] aorta,[12] ovine forestomach derived scaffold materials,[13] and leather made from animal skins.[14] The arrangement of collagen fibrils in most tissues is anisotropic due to the nonuniform requirements for mechanical performance. It has been shown that leather's tear strength is correlated with collagen fibril orientation as measured by SAXS with the X-ray beam edge-on to the sample. Specifically, when the collagen fibrils are arranged in parallel or almost-parallel sheets (i.e., have a high OI), the leather is stronger,[15,16] although OI is also affected by the swelling of the material.[17] This relationship was observed in a large sample of ovine and bovine

Received: July 21, 2015
Accepted: September 3, 2015
Published: September 3, 2015

DOI: 10.1021/acsbiomaterials.5b00310
ACS Biomater. Sci. Eng. 2015, 1, 1026−1038

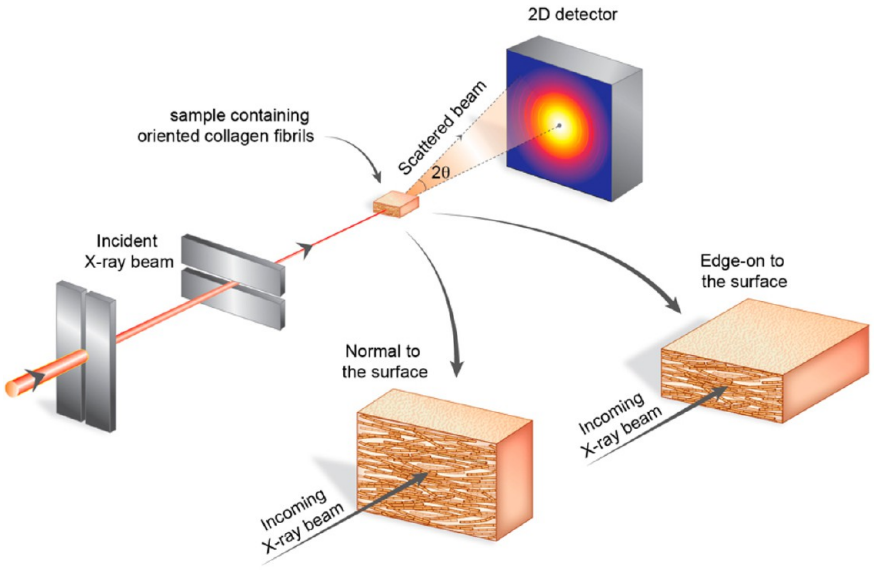

Figure 1. Experimental setup for SAXS analysis.

skins, including bovine pericardium,[8] and across seven species of mammals over a large range of strength (factor of 5). The relationship between OI and strength has been explained as being due to the high strength of the collagen fibrils in their longitudinal axis when suitably arranged to resist the tearing process.[16]

d-Spacing in collagen varies with animal age,[18,19] animal species[16] and tissue type,[20] and the tissue's chemical treatment including water and fat content.[19,21−24] However, there does not appear to be a relationship between *d*-spacing and the strength of leather[15,16] or rat tail tendon.[25]

Collagen fibril diameter may be correlated with strength in some materials. For example, in human aortic valves, regions of high stress may contain larger-diameter fibrils;[26] in mouse tendon, fibril diameter increases with loading;[27] and in bovine leather, higher strength material has larger fibril diameters.[28] Fibril diameter may also increase with age.[29]

Here, we investigate the structure of acellular dermal matrix (ADM) materials, how it differs between bovine, porcine and human materials, and how it changes with age in bovine materials. We attempt to develop an understanding of how ADM structure influences the physical properties of the materials.

EXPERIMENTAL SECTION

Source Material. Commercial ADM materials included Strattice Firm porcine ADM (LifeCell Corporation, US), Alloderm human ADM (LifeCell Corporation, US) and a range of SurgiMend bovine ADM (TEI Biosciences, US), including bovine third trimester fetal ADM and neonatal ADM (animals less than 5 months old) with thicknesses of approximately 1.7, 2.0, 3.0, and 4.0 mm. The Strattice and Alloderm materials were already hydrated whereas the SurgiMend materials required hydrating with distilled water prior to SAXS analysis or tensile testing.

Synchrotron SAXS. Diffraction patterns were recorded on the Australian Synchrotron SAXS/WAXS beamline, using a high-intensity undulator source. Energy resolution of 10^{-4} was obtained from a cryo-cooled Si(111) double-crystal monochromator and the beam size (fwhm focused at the sample) was 250 × 80 μm, with a total photon flux of about 2×10^{12} ph.s^{-1}. All diffraction patterns were recorded with an X-ray energy of 12 keV using a Pilatus 1 M detector with an active area of 170 × 170 mm and a sample-to-detector distance of 3371 mm. Exposure time for diffraction patterns was 1−5 s and initial data processing was carried out using Scatterbrain software.[30]

SAXS analysis was carried out in two directions through the samples. The X-ray beam was either passed through the flat surface of the sample normal to the surface (here referred to as normal) or edge-on to the sample (here referred to as edge-on or cross sections) (Figure 1). For the edge-on measurements, because it is known that structure varies through the thickness of a sample, structure was analyzed at intervals of typically 0.15 mm through the whole thickness of each sample.

Fibril Diameter. Fibril diameters were calculated from the SAXS data using the Irena software package[31] running within Igor Pro. The data were fitted at the wave vector, Q, in the range of 0.01−0.04 Å^{-1} and at an azimuthal angle which was 92.5° (over a 5° segment) to the long axis of most of the collagen fibrils. This azimuthal angle of the long axis of the collagen fibrils was determined as the position for the maximum intensity with azimuthal angle of the *d*-spacing diffraction peaks. The "cylinderAR" shape model with an arbitrary aspect ratio of 30 was used for all fitting. We did not attempt to individually optimize this aspect ratio, and the unbranched length of collagen fibrils may in practice exceed an aspect ratio of 30.

***d*-Spacing.** The *d*-spacing was determined from the position of the center of a Gaussian curve fitted to the fifth order diffraction peak taken from the integrated intensity from the azimuthal range from 45 to 135°.

Orientation Index. The OI is a quantification of the spread of microfibril orientation, with 1 indicating parallel microfibrils and 0 indicating randomly oriented microfibrils. OI is defined as (90° − OA)/90°, where OA, the orientation angle, is the minimum azimuthal angle range that contains 50% of the microfibrils[32] converted to an index,[15] using the spread in azimuthal angle of one or more *d*-spacing diffraction peaks. The peak area is measured, above a fitted baseline, at each azimuthal angle.

In many of the diffraction patterns, particularly those measured with the X-ray beam perpendicular to the surface, two peaks were observed in the plot of intensity versus azimuthal angle. In such patterns, an OA calculated using the minimum angle centered on one of these peaks is large and depends on the spacing between the two peaks, therefore not reflecting accurately the isotropy of the collagen fibrils. So, an alternative method to measure the OA was used: the intensities of 5° intervals of azimuthal angle were ranked and sufficient of these were summed to give 50% of the total intensity over a 180° range, where the total angle covered by the summed intervals becomes the OA. When there is only one peak in the intensity versus azimuthal angle plot, this method gives the same OA as when the OA is calculated by summing the area starting at the center of the peak.[15] Another way of describing this is that the OA for one peak is equivalent to 0.675 of the standard deviation of a

DOI: 10.1021/acsbiomaterials.5b00310
ACS Biomater. Sci. Eng. 2015, 1, 1026−1038

Gaussian (if the peak were approximately Gaussian in shape). When there are two peaks, the standard method of finding a combined standard deviation from two Gaussians to obtain a single OI value would not give a good measure of anisotropy since it depends on the separation of the two Gaussians. A more useful way would be to combine the two Gaussians after shifting them so that they are superimposed. This is effectively what the method used here achieves in a numerical way that is not reliant on Gaussian distributions.

Mechanical Testing. Tear strength[33] and tensile strength[34] were measured using standard methods on an Instron device. Two samples were tested for each of tear strength and tensile strength, with the samples taken orthogonally, and the values averaged.

Electron Microscopy. Samples of ADM materials were cut into small cube-shaped pieces and fixed for over 8 h at room temperature in Modified Karnovsky's fixative containing 3% glutaraldehyde and 2% formaldehyde in 0.1 M phosphate buffer (pH 7.2). The samples were then washed three times for 10−15 min in phosphate buffer (0.1 M, pH 7.2) before being dehydrated in a graded series of ethanol washes (25, 50, 75, 95, and 100%), each dehydration stage being 10−15 min long, followed by a final 100% ethanol wash for 1 h. Samples were critical-point (CP) dried using the Polaron E3000 series II critical point drying apparatus with liquid CO_2 as the CP fluid and 100% ethanol as the intermediary fluid. They were then mounted on to aluminum stubs and sputter coated with gold using the Baltec SCD 050 sputter coater. The samples were viewed in the FEI Quanta 200 environmental scanning electron microscope at an accelerating voltage of 20 kV.

RESULTS

Tear Test. Tear tests were performed in two orthogonal directions for each sample, one test in each direction. The results of these tests have been averaged and are listed in Table 1. The nature of the tearing, once tearing starts, is similar for all the samples.

Table 1. Tear Test Results for ADM Materials

sample	thickness (mm)	force at rupture (N)	σ (for force at rupture, N)	thickness-normalized force at rupture (N/mm)
bovine fetal	0.98	76.1	9.0	78.0
bovine neonatal 1.7	1.67	127.0	0.6	76.0
bovine neonatal 2.0	2.01	172.0	11.7	85.6
bovine neonatal 3.0	3.02	227.0	22.8	75.1
bovine neonatal 4.0	3.98	494.3	0.4	124.2
porcine	1.69	73.0	7.9	43.2
human	1.01	79.5	5.9	79.0

The neonatal bovine ADM materials are the strongest on an absolute scale, followed by the human, the fetal bovine and then the porcine material. On a thickness-normalized scale, the fetal bovine material is the strongest followed by the thicker neonatal bovine materials, with the thinner neonatal bovine having a lower strength in the same range as the human ADM. The lowest strength material on a thickness-normalized basis is the porcine ADM. This may be a partial explanation for the higher intraoperative device failures observed for the porcine cohort in study of porcine and bovine matrix for abdominal wall reconstruction.[35]

Table 2. Tensile Test Results for ADM Materials

sample	thickness[a] (mm)	average force at rupture (N)	σ (for force at rupture, N)	cross-section normalized force at rupture (N/mm^2)
bovine fetal	0.97	381[b]		39.3[b]
bovine neonatal 1.7	1.76	415	111	23.8
bovine neonatal 2.0	2.01	451	147	22.4
bovine neonatal 3.0	3.04	561	6	18.5
bovine neonatal 4.0	4.06	> 963[c]		> 23.7[c]
porcine	1.57	328	7	21.0
human	1.11	201	120	17.7

[a]Some of the thicknesses vary a little from the values in Table 1 but represent the thickness as measured on the cut samples used in each of these tests. [b]Only one test, but see text. [c]Sample was not taken to failure.

Table 3. Strain (approximate) of different sample types

sample	strain at 10 N/mm^2 stress
bovine neonatal 1.7	0.48
bovine neonatal 2.0	0.54
bovine neonatal 3.0	0.47
bovine neonatal 4.0	0.30
porcine	0.31
human	0.45

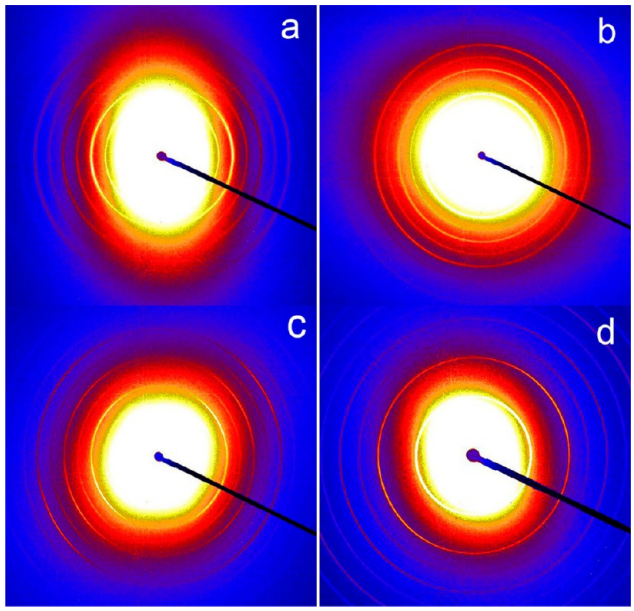

Figure 2. Examples of scattering patterns taken with the X-ray beam edge-on to the samples: (a) fetal bovine; (b) 3 mm thick neonatal bovine; (c) porcine; (d) human ADM materials.

Tensile Test. Tensile tests were performed in two orthogonal directions for each sample, one test in each direction and the averages are listed in Table 2. In the bovine samples, strength increases with thickness; however, the fetal material was the strongest on a thickness-normalized basis. Although not

DOI: 10.1021/acsbiomaterials.5b00310
ACS Biomater. Sci. Eng. 2015, 1, 1026−1038

Table 4. Orientation Index for Collagen from SAXS Measured with the X-ray Beam Edge-on

sample	OI (X-rays edge-on)	σ	no. of measurements
bovine fetal	0.43	0.08	24
bovine neonatal 1.7	0.27	0.06	22
bovine neonatal 2.0	0.32	0.13	22
bovine neonatal 3.0	0.31	0.11	25
bovine neonatal 4.0	0.45	0.15	29
porcine	0.40	0.05	29
human	0.23	0.08	24

Table 5. Orientation Index for Collagen from SAXS Measured with the X-ray Beam Perpendicular to the Surface

sample	OI (X-rays perpendicular)	σ	no. of measurements
bovine fetal	0.24	0.04	18
bovine neonatal 1.7	0.21	0.06	9
bovine neonatal 2.0	0.20	0.07	9
bovine neonatal 3.0	0.14	0.03	9
bovine neonatal 4.0	0.19	0.05	9
porcine	0.61	0.05	9
human	0.08	0.06	9

presented here, a large number of measurements have been made by others on these materials which confirms that the bovine fetal material typically has a higher cross-section-normalized tensile strength than bovine neonatal material.[36]

Extensibility. Extensibility can be approximated as the strain at a force of 10 N/mm^2 on a sample cross section (which is similar to an inverse of elastic modulus over the complete extension range but not thickness normalized). The test results show that the 1.7, 2.0, and 3.0 mm bovine neonatal and human materials are the most extensible, whereas the porcine and 4.0 mm neonatal bovine are the least extensible at this level of force (Table 3).

Small-Angle X-ray Scattering. The SAXS diffraction patterns (Figure 2) can be analyzed in different ways to get structural information on the collagen. The patterns provide information on the structure of the fibrils (*d*-spacing and fibril diameter) and on the arrangement of these fibrils (OI).

Collagen Fibril Orientation Index (OI). Collagen fibril orientation was measured with the X-ray beam edge-on to the ADM materials and perpendicular to the face of the ADM. The OI measured for each material is listed in Tables 4 and 5.

A pairwise multiple comparison of the edge-on measurements (Dunn Method) gave significant differences ($P < 0.05$) between human and both the bovine and porcine ADM materials; between porcine with both human and bovine materials; and between fetal bovine and neonatal bovine. No significant difference in OI was seen when comparing neonatal bovine with either porcine or human.

A pairwise multiple comparison of the flat-on measurements (Dunn Method) gave significant differences ($P < 0.05$) between human and the porcine ADM materials; porcine and both the bovine and human.

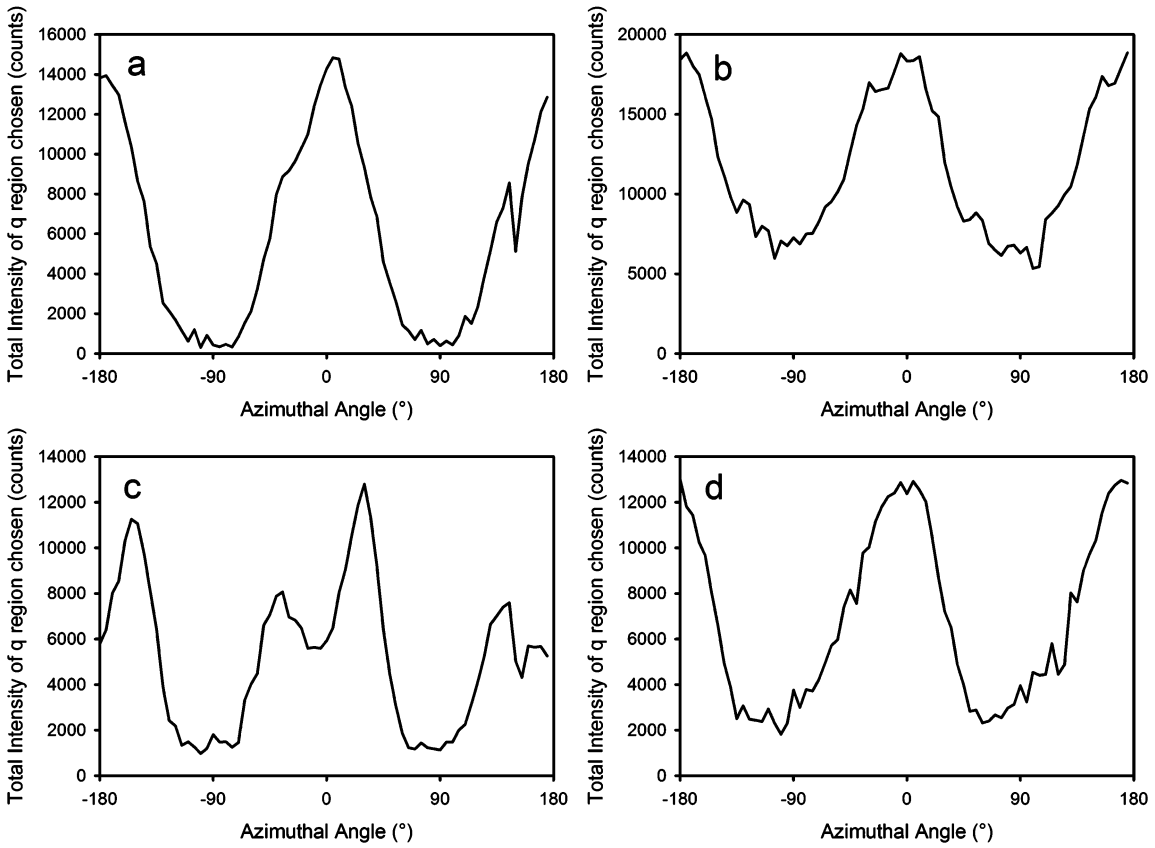

Figure 3. Variation in intensity of the 5th diffraction peak with azimuthal angle (measured with the X-ray beam edge-on to the surface) to illustrate the nature of the fibril orientation: (a) fetal bovine ADM material; (b) 3 mm thick neonatal bovine; (c) porcine; (d) human. These plots correspond with the diffraction patterns in Figure 2.

DOI: 10.1021/acsbiomaterials.5b00310
ACS Biomater. Sci. Eng. 2015, 1, 1026−1038

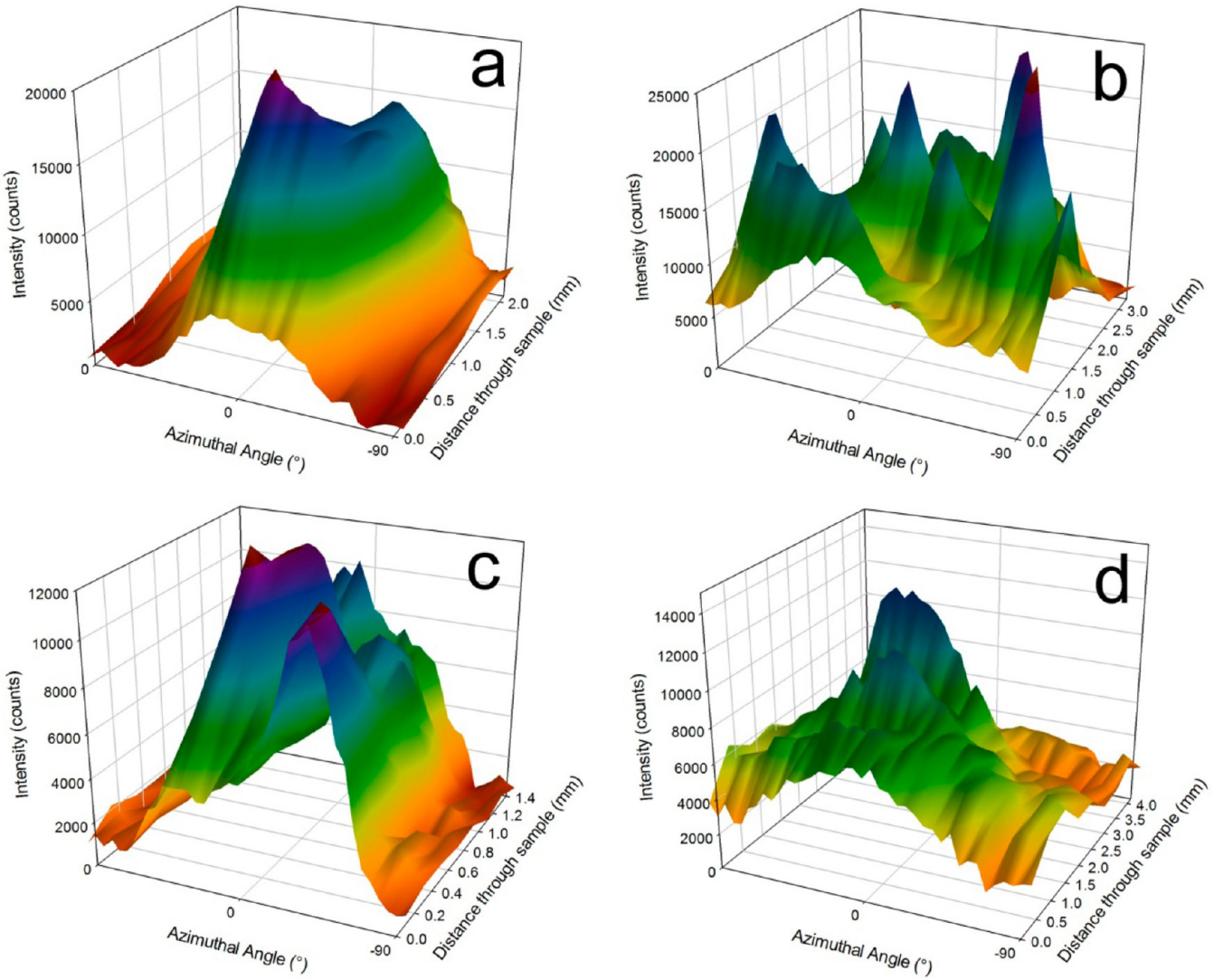

Figure 4. Variation in intensity of the 5th diffraction peak with azimuthal angle (measured with the X-ray beam edge-on to the surface) and distance through the sample (equivalent to a series of plots of the type in Figure 3) to illustrate the nature of the fibril orientation through the sample thickness: a) fetal bovine ADM material; (b) 3 mm thick neonatal bovine; (c) porcine; (d) human. These plots are just for 90° either side of the origin to simplify the images because the information is duplicated in the region for 90 to 180° and −90 to −180°.

Detail of Fibril Orientation. The OI presented for each of the materials is calculated from plots of diffraction intensity for the fifth or sixth *d*-spacing diffraction peak (Figures 3−5); however, the calculation reduces complex information to just one number. More detail of the collagen fibril orientation and the differences between different sample types can be obtained from plots of diffraction intensity (for any of the *d*-spacing diffraction peaks) with azimuthal angle. An analysis of the three-dimensional structure requires at least two diffraction patterns normal to each other. Plots are provided for diffraction intensity versus azimuthal angle with the X-rays edge-on (Figures 3 and 4) and perpendicular (Figure 5) to the plane of the ADM material.

Fibril Orientation (X-rays edge-on). The distribution of orientation of the collagen fibrils in the dermal ECM materials is apparent from the diffraction intensity versus azimuthal angle plots. Single plots at just one point in a section of the ADM are shown in Figure 3. The way the diffraction intensity varies with azimuthal angle gives an indication of how the collagen fibrils are arranged. Where there is only one peak (within a 180° range) and the curve approaches the baseline, there is only one preferred direction of orientation and the spread of fibril direction is around this angle. Examples of this are the edge-on measurements for fetal bovine ADM material (Figure 3a) and to a lesser extent edge-on measurements for neonatal bovine ADM (Figure 3b) and human ADM materials (Figure 3d). Where there are two peaks in this plot, there are two preferred directions of orientation of the collagen fibrils, as seen in the porcine ADM with X-rays edge-on (Figure 3c). When the curve remains considerably above the baseline, the collagen fibril distribution is tending toward isotropic.

Fibril Orientation Sections (X-rays Edge-on). The distribution of orientation of the collagen fibrils and the variation of fibril orientation through the thickness of the ECM materials can be shown with plots of diffraction peak intensity versus azimuthal angle at points at different positions on a cross section of the material representing different depths (Figure 4). These are essentially compilations of plots such as in Figure 3 but with just a −90° to 90° range for simplicity. There is some variation in the fibril arrangement with depth. The bovine, especially fetal, and human materials tend to be a little more highly oriented with

DOI: 10.1021/acsbiomaterials.5b00310
ACS Biomater. Sci. Eng. 2015, 1, 1026−1038

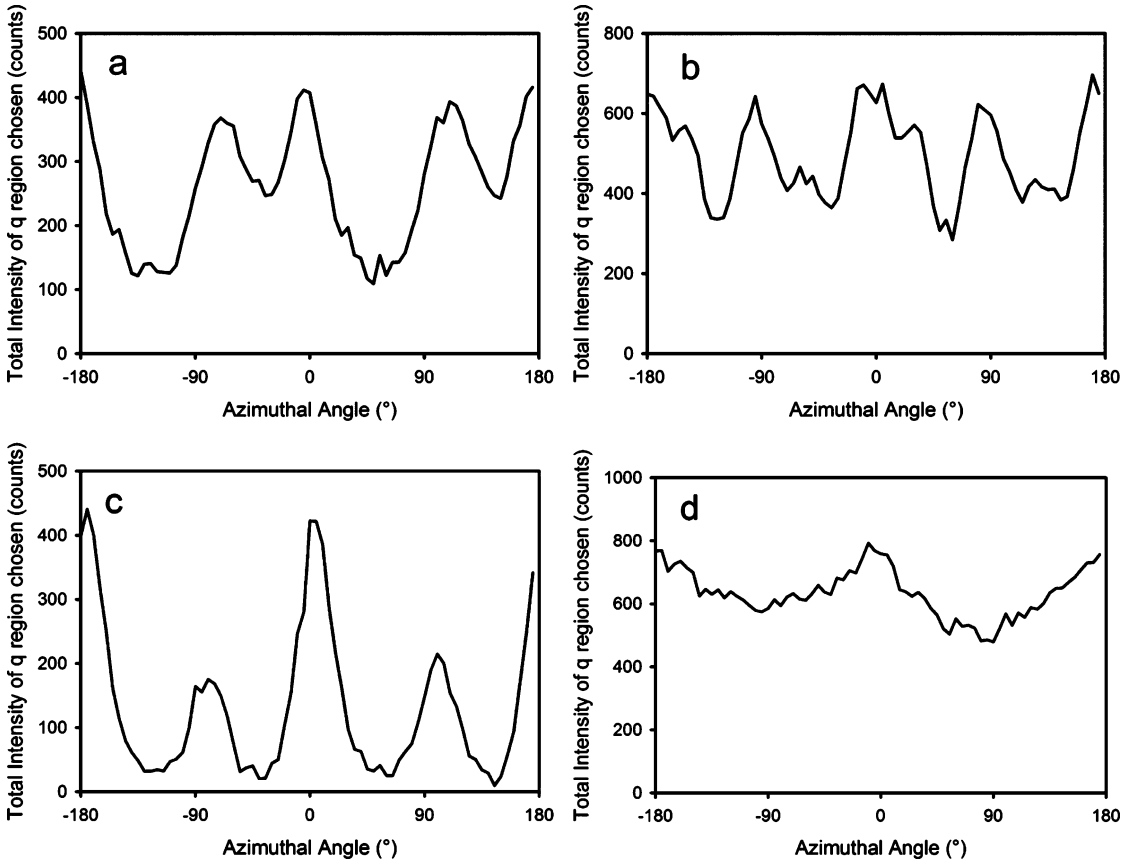

Figure 5. Variation in intensity of the 5th diffraction peak with azimuthal angle (measured with the X-ray beam perpendicular to the surface) to illustrate the nature of fibril orientation: (a) fetal bovine ADM material; (b) 3 mm thick neonatal bovine; (c) porcine; (d) human.

increasing depth. The porcine is highly oriented throughout the thickness, although the direction of orientation changes with depth.

Fibril Orientation (X-rays Normal). Measurements with the X-ray beam perpendicular to the surface reveal differences in fibril orientation between sample types (Figure 5). When the curve remains a long way above the baseline this indicates a tendency toward an isotropic distribution of the collagen fibrils, The fetal bovine ADM material has two well-defined peaks of similar intensity (Figure 5a), as does the neonatal bovine (Figure 5b) although with greater spread and both remaining well above the baseline. The porcine material also has two peaks (Figure 5c), but these are more separate than those of the bovine material (roughly 90° to each other), with one direction dominant, and the curve approaches close to the baseline, showing that the material is far from isotropic. The plots of the human ADM material (Figure 5d) reveal that the fibrils barely exhibit a preferred orientation and are not bimodally distributed.

OI Cross-Sections of ADM. The cross sections through the thickness of the ADM materials (Figure 6) show a variation in OI through the thickness of the bovine materials which, unsurprisingly, is similar to that observed in bovine leather.[37] The fetal bovine material (Figure 6a) is similar to the neonatal material (Figure 6b–e). In the porcine (Figure 6f) and human (Figure 6g) materials, OI varies less through the samples.

Fibril Diameter. Average collagen fibril diameters for each of the sample types calculated from X-ray edge-on measurements are listed in Table 6. A pairwise multiple comparison (Dunn Method) gave significant differences ($P < 0.05$) between porcine and both the human and bovine as well as between human and both the porcine and bovine (except neonatal 3.0). The fetal bovine is not statistically different from the neonatal bovine.

Fetal collagen (rat tail tendon) has been reported to have smaller fibril diameters than collagen from mature animals[29] but we do not observe a difference in collagen fibril diameter between fetal and neonatal bovine ADM materials.

***d*-Spacing.** Average *d*-spacing for the collagen fibrils for each of the sample types is listed in Table 7. A pairwise multiple comparison (Dunn Method) gave significant differences ($P < 0.05$) between human and both the bovine and porcine; porcine and the bovine (except 4.0 mm); porcine and human; but not between fetal bovine and the neonatal bovine.

***d*-Spacing Cross-Sections of ADM.** The *d*-spacing variation through the cross sections is similar for all samples except for the 4 mm neonatal bovine material (Figure 7). The variation between sections is greater for the human, porcine and 4 mm neonatal bovine than for the thinner bovine samples.

Correlation of OI and Strength. Based on measurements with the X-ray beam edge-on to the sample, a statistically significant correlation was found only between OI and tear strength (Figure 8); tensile strength is not significantly correlated with OI (Figure 8 right). These findings are consistent with observations for leather.[15]

For the OI versus tear strength and OI versus tensile strength measured with the X-ray beam perpendicular to the samples there is no statistically significant correlation (Figure 9).

Fibril Diameter and Strength. Fibril diameter has been shown to correlated with tear strength in bovine leather.[28] In collagen grown in tissue culture, larger fibril diameters are associated with higher strength.[38] However, in the bovine

DOI: 10.1021/acsbiomaterials.5b00310
ACS Biomater. Sci. Eng. 2015, 1, 1026–1038

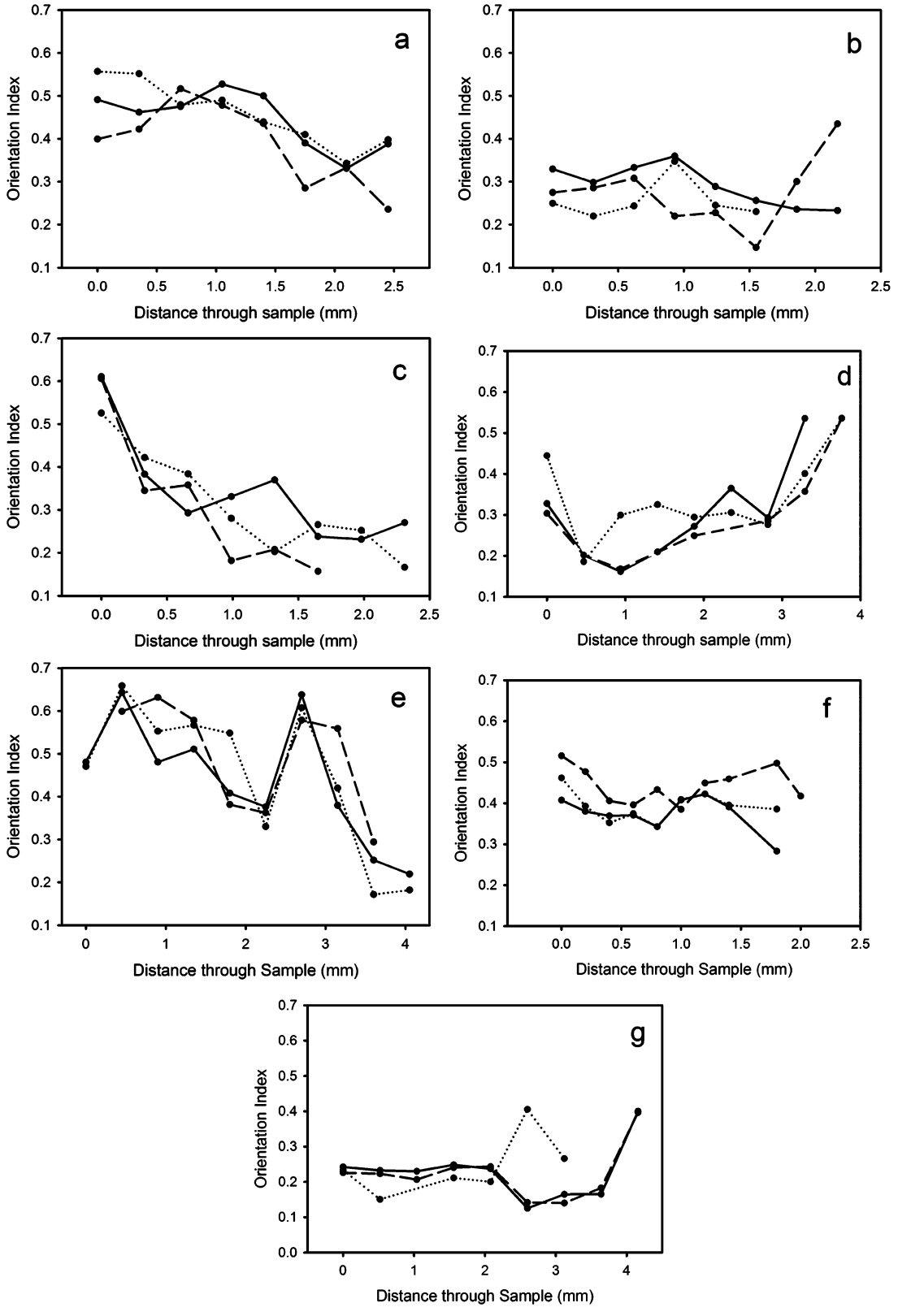

Figure 6. Variation in OI through the thickness of the materials: (a) fetal bovine ADM material; (b) 1.7 mm thick neonatal bovine; (c) 2 mm thick neonatal bovine; (d) 3 mm thick neonatal bovine; (e) 4 mm thick neonatal bovine; (f) porcine; (g) human.

neonatal material we analyzed here, there is no statistically significant correlation between fibril diameter and strength (Figure 10). There is also no correlation in the material of the other species investigated (Figure 10).

SEM Images. The SEM images show structural differences between the bovine, porcine and human ADM (Figures 11 and 12). The bovine material has a more open structure than the porcine and human material, which have a much finer texture.

DOI: 10.1021/acsbiomaterials.5b00310
ACS Biomater. Sci. Eng. 2015, 1, 1026−1038

Table 6. Average Diameter of Collagen Fibrils from SAXS Analysis

sample	fibril diameter (nm)	variance σ	no. of measurements
bovine fetal	58.6	1.3	28
bovine neonatal 1.7	58.3	1.7	26
bovine neonatal 2.0	60.8	1.9	26
bovine neonatal 3.0	57.1	2.5	29
bovine neonatal 4.0	56.0	8.2	32
porcine	61.1	2.1	28
human	55.2	2.7	30

Table 7. Average *d*-Spacing for Collagen from SAXS Analysis (on Hydrated Materials)

sample	*d*-spacing	no. of measurements
bovine fetal	64.00	24
bovine neonatal 1.7	64.13	22
bovine neonatal 2.0	63.95	23
bovine neonatal 3.0	64.01	25
bovine neonatal 4.0	64.23	29
porcine	64.20	28
human	64.60	25

DISCUSSION

Strength from Structure. Collagen structure, as determined by SAXS, is related to the tear strength of the materials. The tear strength differences among bovine pericardium materials are correlated with differences in the collagen fibril orientation index of those materials (Figure 8a). In stronger samples, the fibrils are oriented in a planar manner parallel to the surface of the material (Figure 13b); in weaker materials, fibrils are less oriented in the planar direction (Figure 13a). Orientation direction, as measured with the X-ray beam perpendicular to the plane of the sheets of ADM (Figure 14), does not however have a strong relationship to strength. This has also been seen in leather produced from bovine hides.[15] However, in the ADM materials here, although this relationship was evident in the bovine materials, fibril orientation is not correlated with strength across species. Therefore, although tear strength might be predictable for given OI in bovine materials, this OI will not be associated with the same strength in porcine or human ADM materials. In contrast, studies on leather of seven mammals found a good correlation between OI measured edge-on and strength (although no correlation was found for alligator leather).[15,16] However, we are not able to confirm whether such an OI–strength relationship holds within a selection of porcine or human ADM materials because we did not analyze a range of samples from the two relevant species.

Model for Strength. The relationship between fibril direction and strength has been modeled previously and it can be shown that the strength is due to the sum of the vector components of the fibrils that lie in the direction of force.[8,16,39] A model orientation index is derived which we will call OÍ to distinguish it from the experimentally measured OI eq 1.

$$\mathrm{OI}' = \frac{\int_0^{2\pi}\int_0^{\pi/2} \cos^4\theta F(\theta,\varphi)\mathrm{d}\theta\mathrm{d}\varphi}{\int_0^{2\pi}\int_0^{\pi/2} F(\theta,\varphi)\mathrm{d}\theta\mathrm{d}\varphi} \quad (1)$$

Where $F(\theta,\phi)$ is the angular distribution function where θ and ϕ are fibril angles orthogonal to each other. We have previously applied this model to collagen orientation in leather produced from the skins of a selection of mammals where it was found to be valid across a wide range of strength[16] and also in collagen in bovine pericardium.[8] Other factors that prevent notch growth during tearing are also important.[5]

Distribution of Fibril Orientation with X-rays Normal. The collagen fibril distribution, as measured with the X-rays normal to the surface, perhaps may influence the properties of the materials in service. Although there is no correlation between tear strength and fibril orientation measured with X-rays normal to the surface (Figure 8b), as also seen with leather,[15] elastic properties may vary with fibril direction when the ADM is not isotropic in this dimension. The materials from the different species have different distributions for fibril orientation. A material with an isotropic distribution might be expected to have uniform mechanical properties in all directions (e.g., human and bovine ADM material) whereas one that has a strong unimodal distribution might be expected to behave quite differently in the direction of the orientation compared with a direction at right angles to the orientation. With a bimodal distribution (e.g., as in porcine or fetal bovine ADM materials), the properties would be expected to be more complex but differ in different directions. Other researchers have found that the elastic properties of fetal bovine material are significantly different parallel to the spine (stronger) compared to those perpendicular to the spine (weaker but more elastic).[36] These differences in mechanical properties with direction, if identified for each piece of the material, perhaps could be used to advantage in the selection of materials in specific surgical cases. A detailed study of directional mechanical properties was not part of this study.

***d*-Spacing and Fibril Diameter.** While there are differences between species for both *d*-spacing and fibril diameter, these differences do not appear to be correlated with strength or elasticity. It is known that *d*-spacing decreases with dehydration;[19,21−24] however, for these measurements, the samples were fully hydrated to reflect the state they would be used in surgical application.

Tight or Open Structure. The SEM cross-sections show that there are differences in the structure of the different materials. The bovine materials have the most open structure, with porosity between the fibers, whereas the human and porcine materials are tighter and more compact. At higher magnification, the human ADM looks slightly similar to the bovine material but with a finer texture with some minor porosity between the fibers visible. It may be that a more open structure helps with the integration of the ADM material in vivo,[40] but further, detailed investigation is required.

Variation through Material Thickness. Both the OI (Figures 4 and 6) and *d*-spacing (Figure 7) vary through the thickness of the ADM materials. In the porcine and human ADM material, OI varies less with thickness than do the bovine materials. For other bovine dermal materials, this variation has been well documented;[37] however, the same information is not available for porcine and human ADM. The human material investigated here may, in fact, not reflect a full-thickness dermal material; if so, any measured variation with thickness would be less than for full-thickness material. The *d*-spacing variation through each cross-section is similar for all samples.

Strength. The tear test provides a measure of the toughness of the ADM material and the results are a useful indicator of the in-service stresses and where failure by tearing or bursting is most likely to occur. The neonatal bovine ADM materials are the strongest of the material types in the tear test on an absolute scale, followed by the human, the fetal bovine and then the

DOI: 10.1021/acsbiomaterials.5b00310
ACS Biomater. Sci. Eng. 2015, 1, 1026−1038

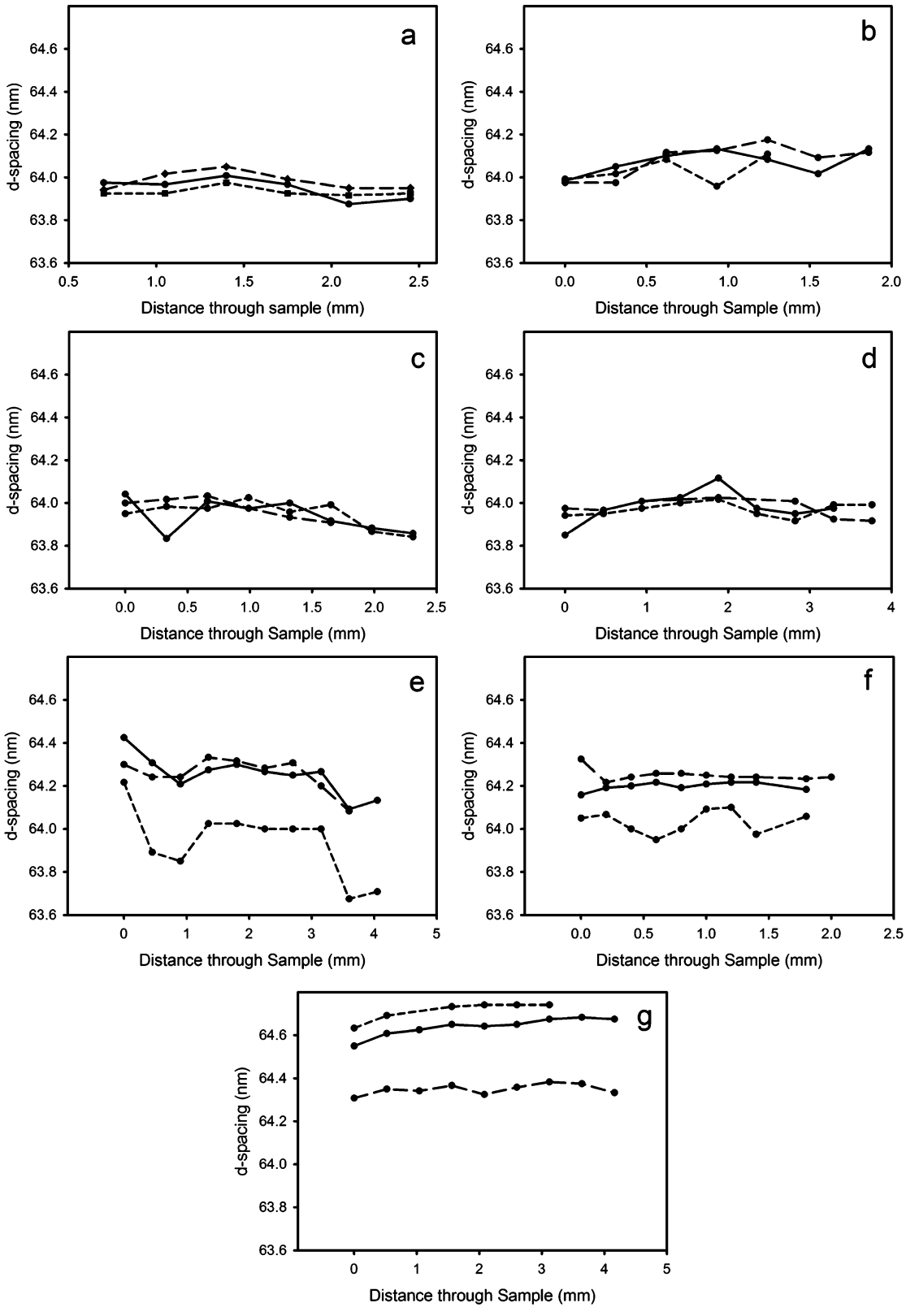

Figure 7. Variation in *d*-spacing through the thickness of ADM materials: (a) fetal bovine, (b) 1.7 mm thick neonatal bovine; (c) 2 mm thick neonatal bovine; (d) 3 mm thick neonatal bovine; (e) 4 mm thick neonatal bovine; (f) porcine; (g) human.

porcine material. The thickness of a surgical scaffold material is also important, partially for aesthetic reasons, and a thin but strong material may be desirable. Therefore, thickness-normalized strength is also a useful measure of the relative merits of different materials. On a thickness-normalized scale, the fetal bovine material is the strongest and its fibers are the most oriented, which perhaps is a general feature of fetal materials (and note that younger bovine pericardium was found to be stronger

DOI: 10.1021/acsbiomaterials.5b00310
ACS Biomater. Sci. Eng. 2015, 1, 1026−1038

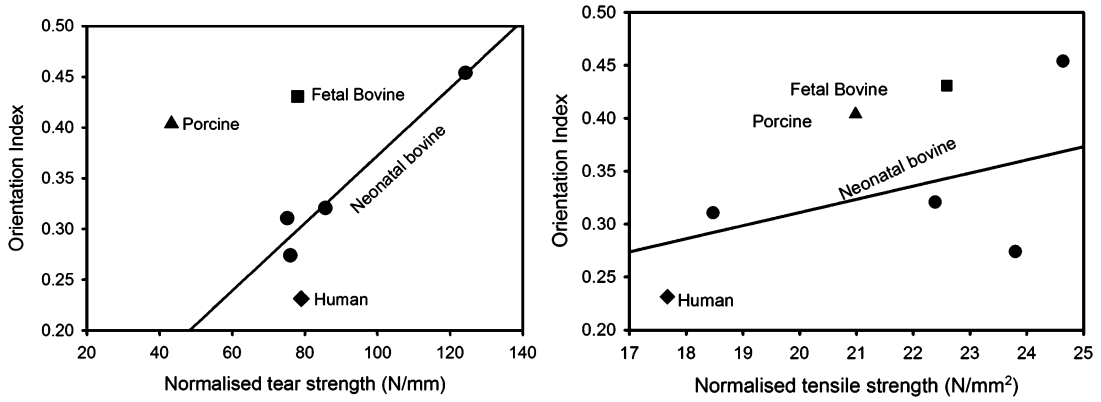

Figure 8. Tear (left) and tensile (right) strength and OI for ADM materials measured with the X-ray beam edge-on to the samples. Line for linear correlation for just the neonatal bovine ADM of varying thickness (tear $r^2 = 0.97$, $P = 0.002$ for $\alpha = 0.05$; tensile $r^2 = 0.44$, $P = 0.22$ for $\alpha = 0.05$).

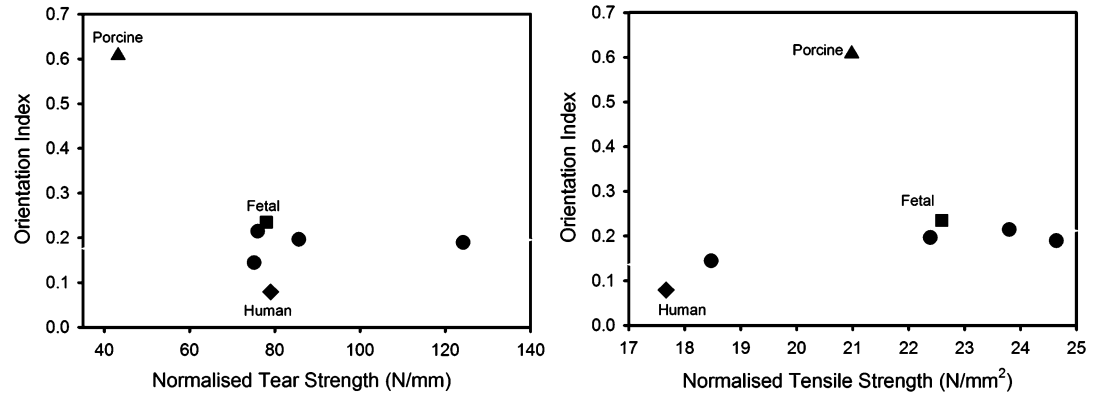

Figure 9. Tear (left) and tensile (right) strength and OI for ADM materials measured with the X-ray beam perpendicular to the samples. Unmarked points are bovine neonatal ADM.

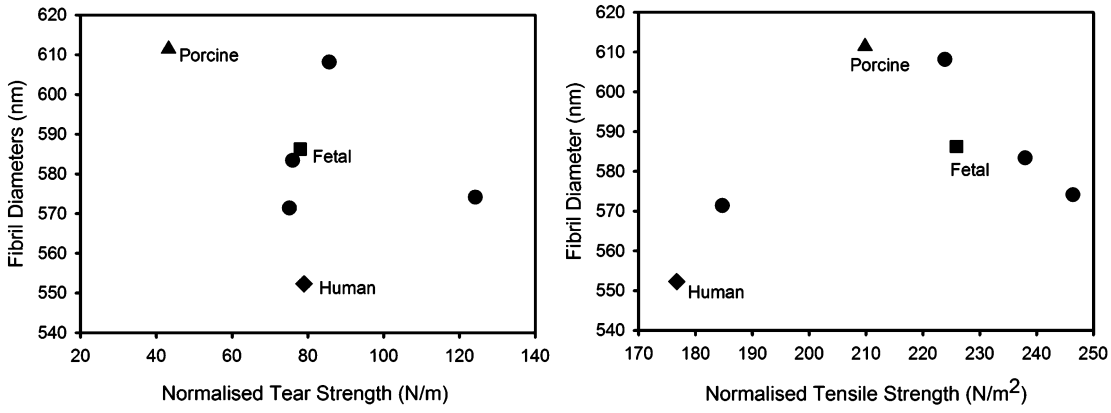

Figure 10. Tear strength and fibril diameter. Unmarked points are bovine neonatal ADM.

than older[8]). The thicker neonatal bovine materials have the next greatest strength, with the thinner neonatal bovine having a lower strength. The strength of these bovine materials is correlated with the OI measured edge-on (Figure 8) as it does in bovine and other leathers.[15,16] In the same strength range as the thinner bovine is the human ADM material, and the lowest strength material on a thickness-normalized basis is the porcine ADM. The strength of the human and porcine ADM material is consistent with the correlation of OI and strength in the bovine materials, so other factors are clearly also important for strength.

These materials derived from different species have largely similar properties and similar structures. There are some differences in strength and in thickness-normalized strength that may provide a preference for one of these materials over others in certain surgical applications. There are also differences in the porosity of the materials, which could be further investigated, quantified, and related to differences in the integration of the scaffold materials in vivo.

CONCLUSIONS

The study of strength and structure of a range of ADM materials has revealed insights into the differences between the materials and the relationship between the structure and some of the physical properties. Bovine ADM material is similar in strength to

DOI: 10.1021/acsbiomaterials.5b00310
ACS Biomater. Sci. Eng. 2015, 1, 1026−1038

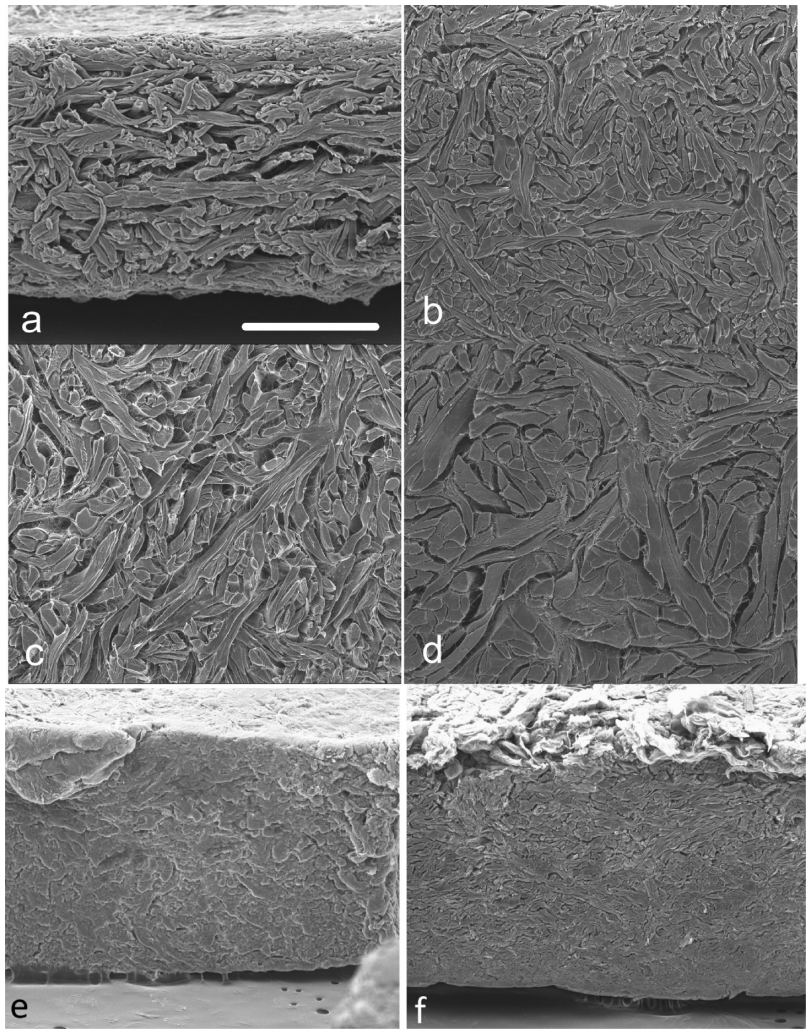

Figure 11. Scanning electron microscopy images through the thickness of the ADM materials: (a) fetal bovine; (b) neonatal bovine 2 mm thick; (c) neonatal bovine 3 mm thick; (d) neonatal bovine 4 mm thick; (e) porcine; (f) human. All at the same magnification; bar is 500 μm.

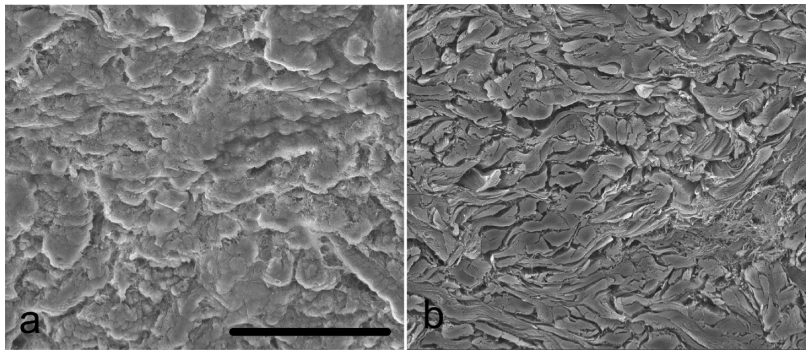

Figure 12. Scanning electron microscopy images at higher magnification through the thickness of the ADM materials: (a) porcine, (b) human. Both at the same magnification; bar is 200 μm.

or a little stronger than human ADM and is significantly stronger than porcine ADM. There is a wide variation in strength in bovine ADM materials and that variation is due to differences in collagen fibril orientation, with stronger materials having a more layered fibril structure. The human ADM material and the thinner (1.7, 2.0, and 3.0 mm) neonatal bovine materials are the most extensible (extensibility to 10 N/mm^2) while the porcine, fetal bovine and 4.0 mm neonatal bovine are the least extensible at this force. Bovine ADM materials have a more open structure than human or porcine ADM and we speculate (however without evidence) that this open structure might help with the integration of the ADM in vivo. The "weft/weave" structures of bovine, porcine and human ADM differ. The human material is the most isotropic, followed by bovine, whereas the porcine is the most anisotropic; these variations may affect the properties of the material in service, although this has not been studied in depth here. It has been shown that there are many similarities in the structures in the different materials but also some subtle

DOI: 10.1021/acsbiomaterials.5b00310
ACS Biomater. Sci. Eng. 2015, 1, 1026−1038

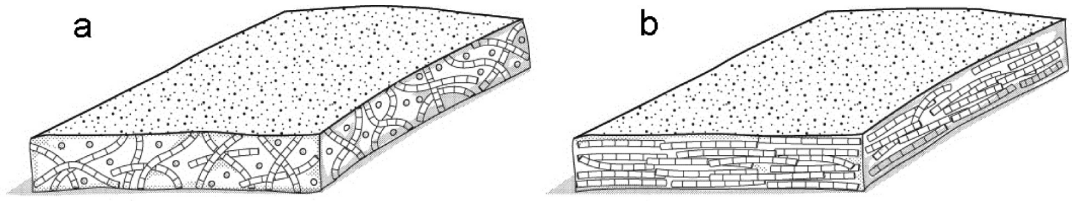

Figure 13. Illustration of the difference between ADM material that is (a) poorly oriented when measured with the X-ray beam edge-on; (b) highly oriented when measured with the X-ray beam edge-on.

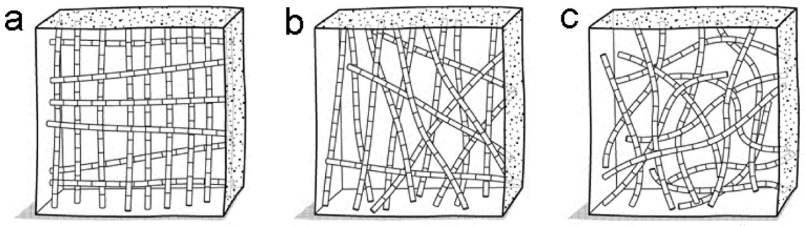

Figure 14. Illustration of the difference between ADM material that is (a) highly oriented in two orthogonal directions when measured with the X-ray beam perpendicular to the sample face, such as in porcine material; (b) partly oriented when measured with the X-ray beam perpendicular to the sample face, such as in bovine material; (c) largely isotropic when measured with the X-ray beam perpendicular to the sample face, such as in human material.

differences which affect physical properties and it may be that the differences in porosity are also important and worth investigating.

AUTHOR INFORMATION

Corresponding Author

*E-mail: r.haverkamp@massey.ac.nz.

Funding

The work was funded in part by the Australian Synchrotron and an unrestricted educational grant from TEI Biosciences.

Notes

The authors declare the following competing financial interest(s): Funding was obtained for this work under an unrestricted educational grant from TEI Biosciences.

ACKNOWLEDGMENTS

This research was undertaken on the SAXS/WAXS beamline at the Australian Synchrotron, Victoria, Australia. The Australian Synchrotron assisted with travel funding and accommodation. This work was supported by a grant from TEI Biosciences. Bret Jessee and Vladimir Russakovsky of TEI Biosciences provided the samples and the motivation for the work. Sue Hallas of Nelson assisted with editing the manuscript.

REFERENCES

(1) Lutolf, M. P.; Hubbell, J. A. Synthetic biomaterials as instructive extracellular microenvironments for morphogenesis in tissue engineering. *Nat. Biotechnol.* **2005**, *23* (1), 47−55.

(2) Badylak, S. F.; Freytes, D. O.; Gilbert, T. W. Extracellular matrix as a biological scaffold material: Structure and function. *Acta Biomater.* **2009**, *5* (1), 1−13.

(3) Meyers, M. A.; McKittrick, J.; Chen, P. Y. Structural biological materials: Critical mechanics-materials connections. *Science* **2013**, *339* (6121), 773−779.

(4) Wells, H. C.; Sizeland, K. H.; Kayed, H. R.; Kirby, N.; Hawley, A.; Mudie, S. T.; Haverkamp, R. G. Poisson's ratio of collagen fibrils measured by SAXS of strained bovine pericardium. *J. Appl. Phys.* **2015**, *117* (4), 044701.

(5) Yang, W.; Sherman, V. R.; Gludovatz, B.; Schaible, E.; Stewart, P.; Ritchie, R. O.; Meyers, M. A. On the tear resistance of skin. *Nat. Commun.* **2015**, *6*, 6649.

(6) Boote, C.; Kamma-Lorger, C. S.; Hayes, S.; Harris, J.; Burghammer, M.; Hiller, J.; Terrill, N. J.; Meek, K. M. Quantification of collagen organization in the peripheral human cornea at micron-scale resolution. *Biophys. J.* **2011**, *101* (1), 33−42.

(7) Sellaro, T. L.; Hildebrand, D.; Lu, Q. J.; Vyavahare, N.; Scott, M.; Sacks, M. S. Effects of collagen fiber orientation on the response of biologically derived soft tissue biomaterials to cyclic loading. *J. Biomed. Mater. Res., Part A* **2007**, *80A* (1), 194−205.

(8) Sizeland, K. H.; Wells, H. C.; Higgins, J. J.; Cunanan, C. M.; Kirby, N.; Hawley, A.; Haverkamp, R. G. Age dependent differences in collagen fibril orientation of glutaraldehyde fixed bovine pericardium. *BioMed Res. Int.* **2014**, *2014*, 189197.

(9) Liao, J.; Yang, L.; Grashow, J.; Sacks, M. S. Molecular orientation of collagen in intact planar connective tissues under biaxial stretch. *Acta Biomater.* **2005**, *1* (1), 45−54.

(10) Gilbert, T. W.; Wognum, S.; Joyce, E. M.; Freytes, D. O.; Sacks, M. S.; Badylak, S. F. Collagen fiber alignment and biaxial mechanical behavior of porcine urinary bladder derived extracellular matrix. *Biomaterials* **2008**, *29* (36), 4775−4782.

(11) Purslow, P. P.; Wess, T. J.; Hukins, D. W. L. Collagen orientation and molecular spacing during creep and stress-relaxation in soft connective tissues. *J. Exp. Biol.* **1998**, *201*, 135−142.

(12) Gasser, T. C. An irreversible constitutive model for fibrous soft biological tissue: A 3-D microfiber approach with demonstrative application to abdominal aortic aneurysms. *Acta Biomater.* **2011**, *7* (6), 2457−2466.

(13) Floden, E. W.; Malak, S.; Basil-Jones, M. M.; Negron, L.; Fisher, J. N.; Byrne, M.; Lun, S.; Dempsey, S. G.; Haverkamp, R. G.; Anderson, I.; Ward, B. R.; May, B. C. H.; et al. Biophysical characterization of ovine forestomach extracellular matrix biomaterials. *J. Biomed. Mater. Res., Part B* **2011**, *96B* (1), 67−75.

(14) Basil-Jones, M. M.; Edmonds, R. L.; Allsop, T. F.; Cooper, S. M.; Holmes, G.; Norris, G. E.; Cookson, D. J.; Kirby, N.; Haverkamp, R. G. Leather structure determination by small-angle X-ray scattering (SAXS): Cross sections of ovine and bovine leather. *J. Agric. Food Chem.* **2010**, *58* (9), 5286−5291.

(15) Basil-Jones, M. M.; Edmonds, R. L.; Cooper, S. M.; Haverkamp, R. G. Collagen fibril orientation in ovine and bovine leather affects strength: A small angle X-ray scattering (SAXS) study. *J. Agric. Food Chem.* **2011**, *59* (18), 9972−9979.

(16) Sizeland, K. H.; Basil-Jones, M. M.; Edmonds, R. L.; Cooper, S. M.; Kirby, N.; Hawley, A.; Haverkamp, R. G. Collagen alignment and leather strength for selected mammals. *J. Agric. Food Chem.* **2013**, *61* (4), 887−892.

DOI: 10.1021/acsbiomaterials.5b00310
ACS Biomater. Sci. Eng. 2015, 1, 1026−1038

(17) Sizeland, K. H.; Edmonds, R. L.; Basil -Jones, M. M.; Kirby, N.; Hawley, A.; Mudie, S.; Haverkamp, R. G. Changes to collagen structure during leather processing. *J. Agric. Food Chem.* **2015**, *63* (9), 2499−2505.
(18) James, V. J.; McConnell, J. F.; Capel, M. The D-spacing of collagen from mitral heart-valves changes with aging, but not with collagen type-III content. *Biochim. Biophys. Acta, Protein Struct. Mol. Enzymol.* **1991**, *1078* (1), 19−22.
(19) Scott, J. E.; Orford, C. R.; Hughes, E. W. Proteoglycan-collagen arrangements in developing rat tail tendon - an electron-microscopical and biochemical investigation. *Biochem. J.* **1981**, *195* (3), 573−584.
(20) Fang, M.; Goldstein, E. L.; Turner, A. S.; Les, C. M.; Orr, B. G.; Fisher, G. J.; Welch, K. B.; Rothman, E. D.; Banaszak Holl, M. M. Type I collagen D-spacing in fibril bundles of dermis, tendon, and bone: Bridging between nano- and micro-level tissue hierachy. *ACS Nano* **2012**, *6*, 9503−9514.
(21) Ripamonti, A.; Roveri, N.; Braga, D.; Hulmes, D. J. S.; Miller, A.; Timmins, P. A. Effects of pH and ionic-strength on the structure of collagen fibrils. *Biopolymers* **1980**, *19* (5), 965−975.
(22) Sizeland, K. H.; Wells, H. C.; Norris, G. E.; Edmonds, R. L.; Kirby, N.; Hawley, A.; Mudie, S.; Haverkamp, R. G. Collagen D-spacing and the effect of fat liquor addition. *J. Am. Leather Chem. Assoc.* **2015**, *110* (3), 66−71.
(23) Wess, T. J.; Orgel, J. P. Changes in collagen structure: drying, dehydrothermal treatment and relation to long term deterioration. *Thermochim. Acta* **2000**, *365* (1−2), 119−128.
(24) Masic, A.; Bertinetti, L.; Schuetz, R.; Chang, S.-W.; Metzger, T. H.; Buehler, M. J.; Fratzl, P. Osmotic pressure induced tensile forces in tendon collagen. *Nat. Commun.* **2015**, *6*, 5942.
(25) Gonzalez, A. D.; Gallant, M. A.; Burr, D. B.; Wallace, J. M. Multiscale analysis of morphology and mechanics in tail tendon from the ZDSD rat model of type 2 diabetes. *J. Biomech.* **2014**, *47*, 681−686.
(26) Balguid, A.; Driessen, N. J.; Mol, A.; Schmitz, J. P. J.; Verheyen, F.; Bouten, C. V. C.; Baaijens, F. P. T. Stress related collagen ultrastructure in human aortic valves - implications for tissue engineering. *J. Biomech.* **2008**, *41* (12), 2612−2617.
(27) Michna, H. Morphometric analysis of loading-induced changes in collagen-fibril populations in young tendons. *Cell Tissue Res.* **1984**, *236* (2), 465−470.
(28) Wells, H. C.; Edmonds, R. L.; Kirby, N.; Hawley, A.; Mudie, S. T.; Haverkamp, R. G. Collagen fibril diameter and leather strength. *J. Agric. Food Chem.* **2013**, *61* (47), 11524−11531.
(29) Parry, D. A. D.; Barnes, G. R. G.; Craig, A. S. Comparison of size distribution of collagen fibrils in connective tissues as a function of age and a possible relation between fibril size distribution and mechanical-properties. P. Roy. *Proc. R. Soc. London, Ser. B* **1978**, *203* (1152), 305−321.
(30) Cookson, D.; Kirby, N.; Knott, R.; Lee, M.; Schultz, D. Strategies for data collection and calibration with a pinhole-geometry SAXS instrument on a synchrotron beamline. *J. Synchrotron Radiat.* **2006**, *13*, 440−444.
(31) Ilavsky, J.; Jemian, P. R. Irena: tool suite for modeling and analysis of small-angle scattering. *J. Appl. Crystallogr.* **2009**, *42*, 347−353.
(32) Sacks, M. S.; Smith, D. B.; Hiester, E. D. A small angle light scattering device for planar connective tissue microstructural analysis. *Ann. Biomed. Eng.* **1997**, *25* (4), 678−689.
(33) Williams, J. M. V. IULTCS (IUP) test methods - Measurement of tear load-double edge tear. *J. Soc. Leather Technol. Ch.* **2000**, *84* (7), 327−329.
(34) Williams, J. M. V. IULTCS (IUP) test methods - Measurement of tensile strength and percentage elongation. *J. Soc. Leather Technol. Ch.* **2000**, *84* (7), 317−321.
(35) Clemens, M. W.; Selber, J. C.; Liu, J.; Adelman, D. M.; Baumann, D. P.; Garvey, P. B.; Butler, C. E. Bovine versus Porcine Acellular Dermal Matrix for Complex Abdominal Wall Reconstruction. *Plastic Reconstruc. Surg.* **2013**, *131* (1), 71−79.
(36) Russakovsky, V. *Personal communication*, 2015.
(37) Basil-Jones, M. M.; Edmonds, R. L.; Norris, G. E.; Haverkamp, R. G. Collagen fibril alignment and deformation during tensile strain of leather: A small-angle X-ray scattering study. *J. Agric. Food Chem.* **2012**, *60*, 1201−1208.
(38) Herchenhan, A.; Bayer, M. L.; Svensson, R. B.; Magnusson, S. P.; Kjaer, M. In vitro tendon tissue development from human fibroblasts demonstrates collagen fibril diameter growth associated with a rise in mechanical strength. *Dev. Dyn.* **2013**, *242* (1), 2−8.
(39) Bigi, A.; Ripamonti, A.; Roveri, N.; Jeronimidis, G.; Purslow, P. P. Collagen orientation by X-Ray pole figures and mechanical-properties of media carotid wall. *J. Mater. Sci.* **1981**, *16* (9), 2557−2562.
(40) Wolf, K.; Alexander, S.; Schacht, V.; Coussens, L. M.; von Andrian, U. H.; van Rheenen, J.; Deryugina, E.; Friedl, P. Collagen-based cell migration models in vitro and in vivo. *Semin. Cell Dev. Biol.* **2009**, *20* (8), 931−941.

DOI: 10.1021/acsbiomaterials.5b00310
ACS Biomater. Sci. Eng. 2015, 1, 1026−1038